The Role of the Plasmasphere in Radiation Belt Particle Energization and Loss

Wm. Robert Johnston

Ph.D. Dissertation Presentation

University of Texas at Dallas

8 April 2009

Outline

- Background
  - plasmasphere, LIT, radiation belts
- Instruments
  - DMSP, IMAGE, SAMPEX
- Method and Results
  - use DMSP observations of LIT to identify plasmapause
  - comparisons with IMAGE, model
  - application to relativistic microbursts
  - application to radiation belt flux dynamics
- Conclusions
- Continuing Research

Magnetosphere and plasmasphere

- Inner magnetosphere
  - Corotating B field, closed drift paths
  - Plasmasphere and radiation belts
- Plasmasphere
  - Cold, dense plasma
  - H+, 5-10% He+
  - Out to L=3-5, dynamic
- Steady state plasmasphere
  - Bounded by transition from corotation/closed drift paths to open drift paths
  - Within PP, flux tubes fill with ionospheric plasma
  - Outside PP, flux tubes convect to magnetopause and empty

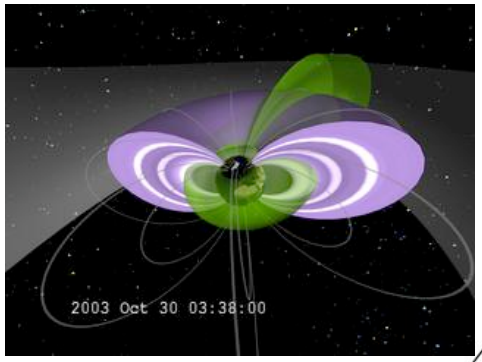

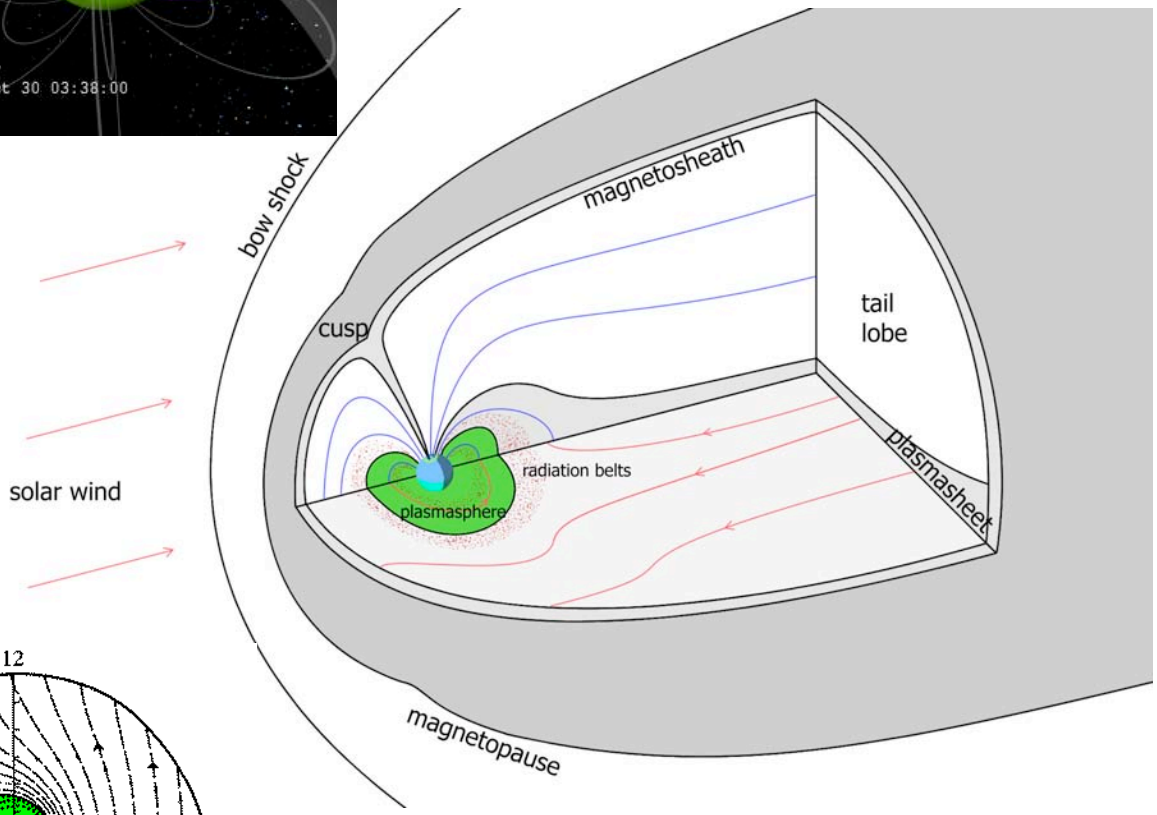

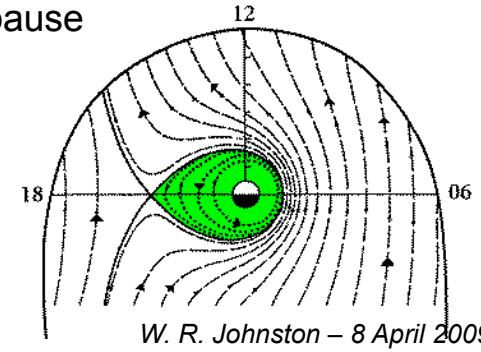

Plasmasphere in stormtime

- Stronger convection field -> contraction, erosion by emptying (hours)
- Weaker convection field -> refilling (days)
- Plasmapause location depends on history, not just convective E-field
- Figure shows IMAGE EUV observations (top), interpretation (bottom)

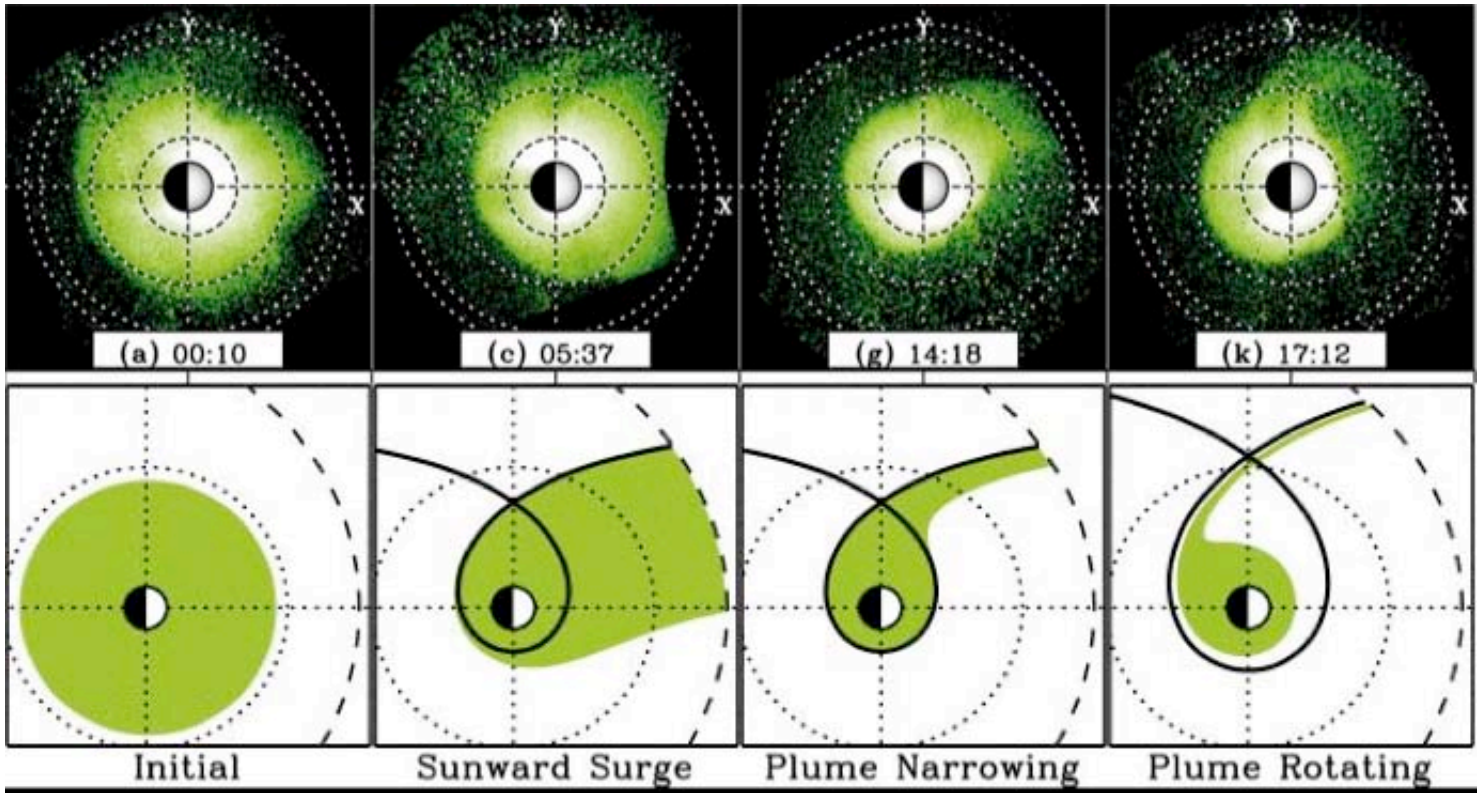

Goldstein (2004) ORBITALS workshop

Plasmapause signatures in ionosphere

- Several ionospheric signatures of the plasmapause have been proposed, including:
  - midlatitude electron density trough - SETE - LIT
  - precipitating electron boundary - SAR arcs
- Generally not a one-to-one correspondence between any of these and the plasmapause
- The light ion trough (LIT) is proposed as one of the more consistent signatures (Taylor and Walsh, 1972, *JGR, 77*:6716; Horwitz et al., 1990, *JGR, 95*:7949)
- Some have found the LIT tends to be equatorward of other plasmapause identifications (Foster et al., 1978, *JGR, 83*:1175) or a possible LIT-plasmapause mismatch on the duskside Grebowsky et al., 1978, *PSS, 26*:651)

Light ion trough

- The light ion trough (LIT) is the region of low ionospheric H^+/He^+ density near the equatorial edge of the auroral zone
- A simple model links the LIT and plasmapause:
  - H^+ escapes from ionosphere due to large scale height/thermal velocity
  - equatorward of LIT, escaping light ions saturate closed flux tubes, forming the plasmasphere
  - poleward of LIT, light ions are on flux tubes that eventually empty through the dayside magnetopause

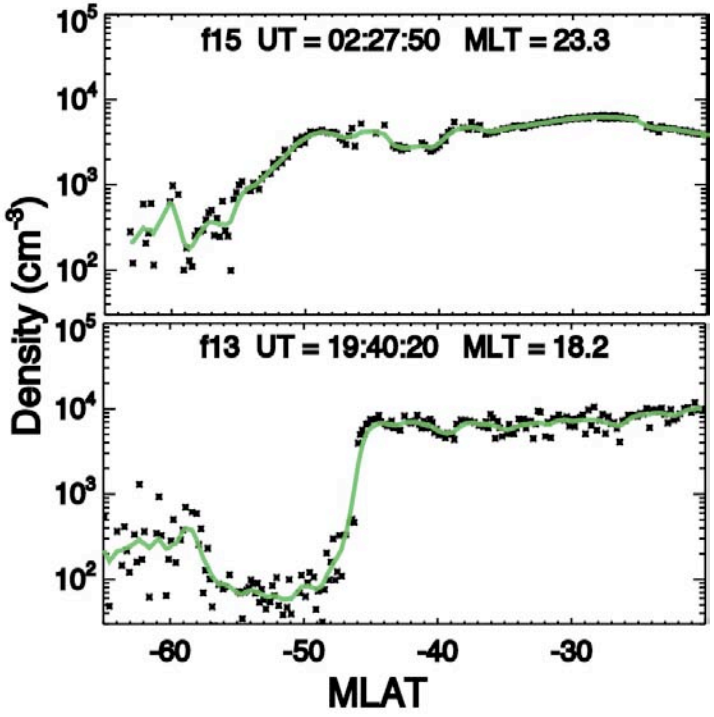

- Reality is more complicated:
  - temperature gradient associated with LIT produces change in scale height: ionospheric density gradient may not be on same field line as the density gradient at high altitude
  - LIT may be generally equatorward of PP due to H^+ outflow, long refilling times for outer PP flux tubes, horizontal E fields (Foster et al., 1978, *JGR*, 83:1175).

Radiation belts

- Radiation belts are comprised of energetic charged particles (keV to MeV) trapped by the Earth's magnetic field
  - two-belt structure, with outer electron belt very dynamic in stormtimes
- Trapped particle motion includes three periodic motions
  - gyromotion, bounce, drift
- Steady-state radiation belts are a dynamic balance of various sources, diffusion mechanisms, and losses
  - including a variety of wave-particle interactions

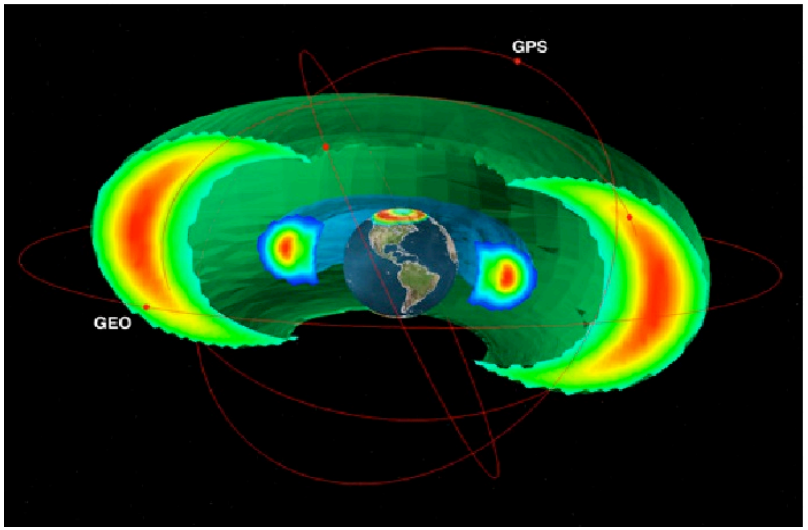

NASA web site

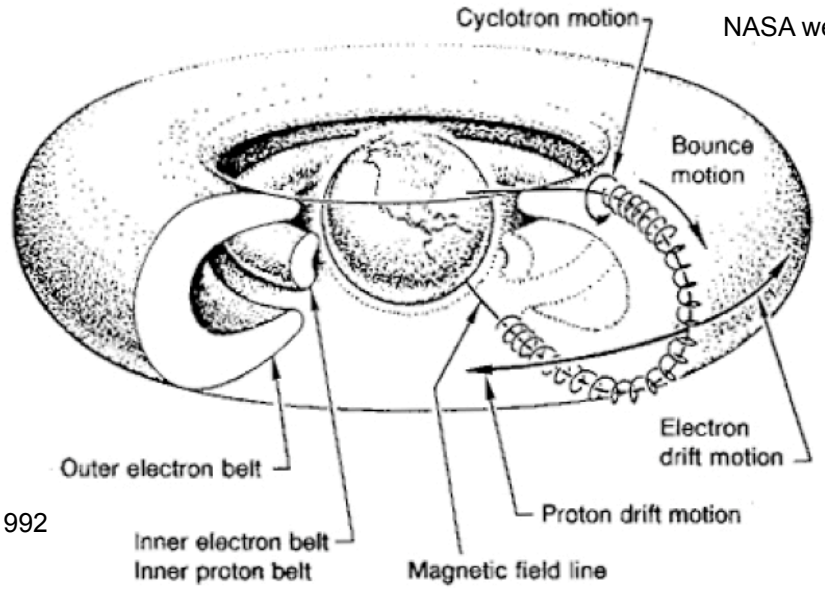

McKay et al., 1992

Plasmasphere-radiation belt connection

- Plasmapause (PP) correlates with inner edge of outer radiation belt
- Wave-particle interactions are proposed as the casual link:
  - stormtime EMIC waves inside duskside PP scatter radiation belt particles into loss cone, rapidly depleting outer belt
  - Significant stormtime losses from chorus-related relativistic microbursts
  - Slower depletion from whistler hiss inside PP
  - whistler-mode chorus outside PP energizes radiation belt particles over multiple orbits, slowly repopulating belt (Summers et al., 1998, *JGR,* 103:20487)

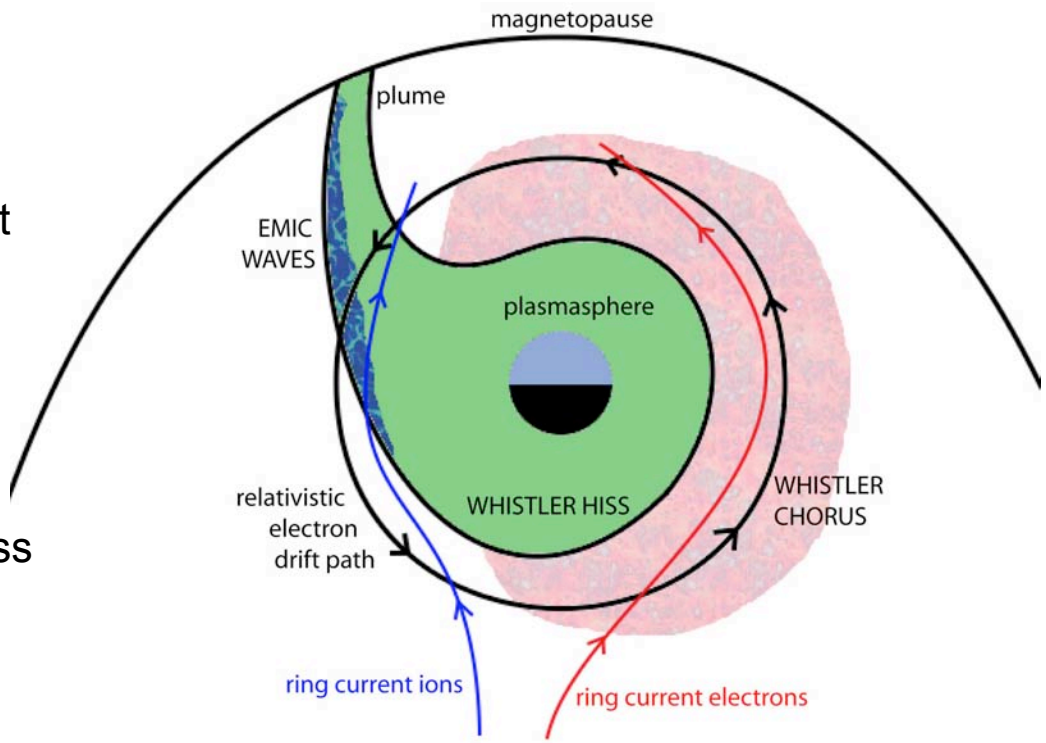

Chorus wave-particle interactions

- Equation for conditions for gyro-resonance between EM waves and electrons →
  - n=1,2,3,... whistler interactions
  - n=0 Landau resonance
  - n=-1 EMIC interaction (relativistic)
- How to make whistler chorus
  - Injections into ring current provide soft electron population (~tens of keV)
  - Pitch-angle-dependent drift and non-dipolar field produce population anisotropies
  - Anisotropies lead to instabilities for wave growth at expense of electron energy
  - Tail end of electron population can gain energy at expense of chorus
  - Individual high amplitude chorus elements can scatter electrons into loss cone—fast
- Whistler chorus is most intense outside the PP on the dawn side and during storms (Meredith et al., 2003, *GRL*, 30:1871).
- Whistler chorus reflected into plasmasphere may be the main source of whistler hiss (Bortnik et al., 2009, *Nature*, 452:62)

$$\omega - k_{\|} v_{\|} = \frac{n|\Omega_e|}{\gamma}$$

$$\gamma = \frac{1}{\sqrt{1-(v/c)^2}}$$

$$\Omega_e = \frac{qB}{m_0}$$

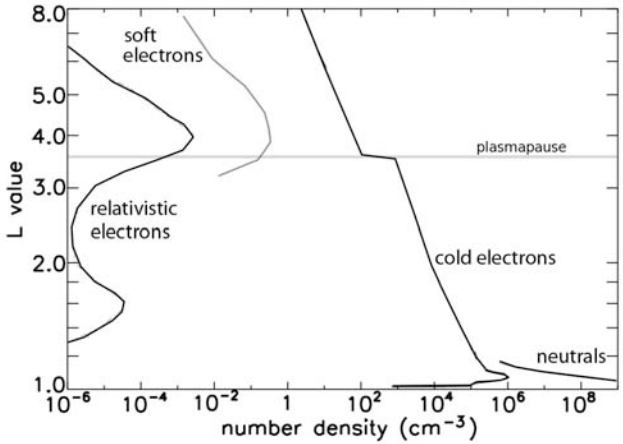

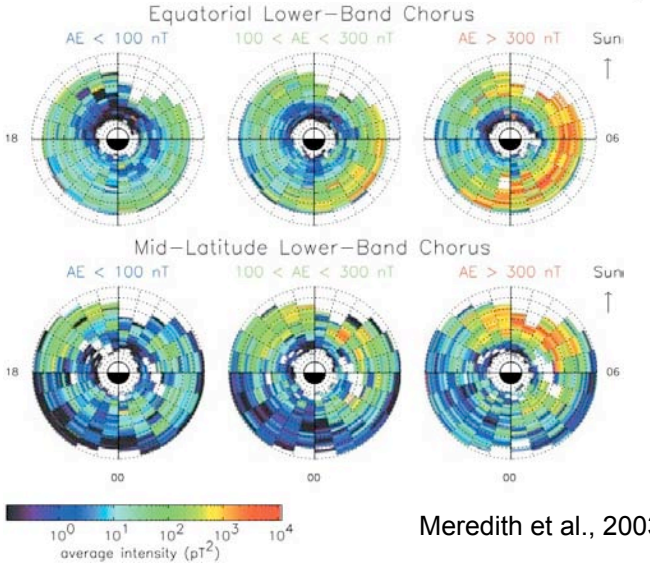

Meredith et al., 2003

Microbursts

- Microbursts: short duration (<1 sec) bursts of precipitating relativistic electrons observed in LEO
  - Distinct from “soft” microbursts
  - First reported by Brown and Stone (1972, JGR, 77:3384)
  - Associated with dawnside and post-storm RB recovery (Nakamura et al., 2000, JGR, 111:A11S02)
  - Innermost occurrences associated with modeled PP location (Lorentzen et al., 2001, GRL, 28:2573)

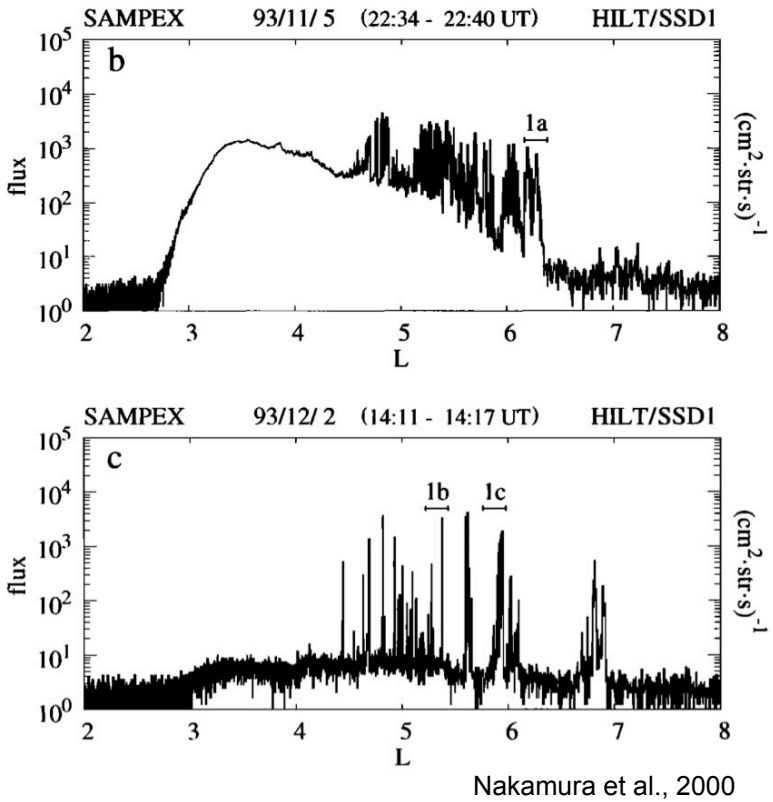

Nakamura et al., 2000

- They are believed to represent wave-particle scattering of RB particles into the loss cone
  - Linked to VLF chorus (Lorentzen et al., 2001, JGR, 106:6017)
  - Side effect of energization by whistler chorus outside PP?
  - Connected to high-amplitude storm-time chorus?

Instruments

DMSP

- DMSP satellites: sun-synchronous circular orbits near 840 km alt., 101 min. period, 99° inclination
- 3-4 satellites in operation continuously over 10+ years
- Plot illustrates polar coverage in one day from four DMSP satellites (F11-F14) in MLAT-MLT
  - provides ~50% MLT coverage at 40°, ~75% coverage at 60°
- Instruments include
  - **RPA:** Retarding Potential Analyzer providing ion density, composition, temperature
  - Ion Drift Meter providing cross track ion velocity
  - SSJ/4 or SSJ/5 providing energy spectra/flux of precipitating electrons and ions

DMSP Coverage October 19, 1998

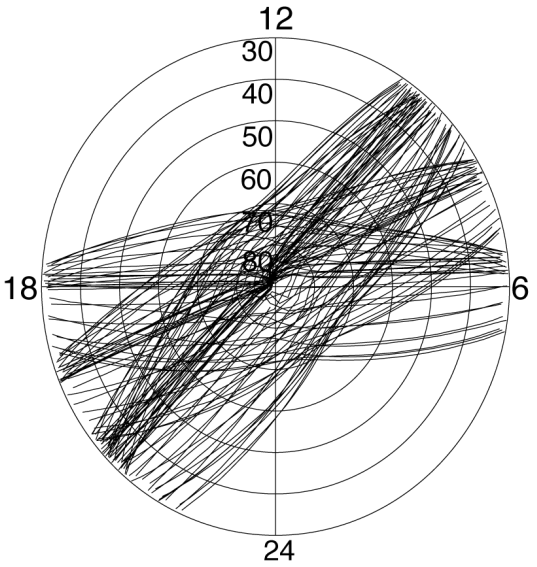

IMAGE

- IMAGE spacecraft:
  - eccentric polar orbit, from 1400 km alt. to 8 R_E
  - operational 3/2000 to 12/2005
- **EUV** imager
  - directly imaged 30.4 nm UV resonantly scattered by He^+
  - could image plasmasphere by its He^+ component
- Sample of extracted plasmapause locations from reprojected EUV image (from J. Goldstein)--

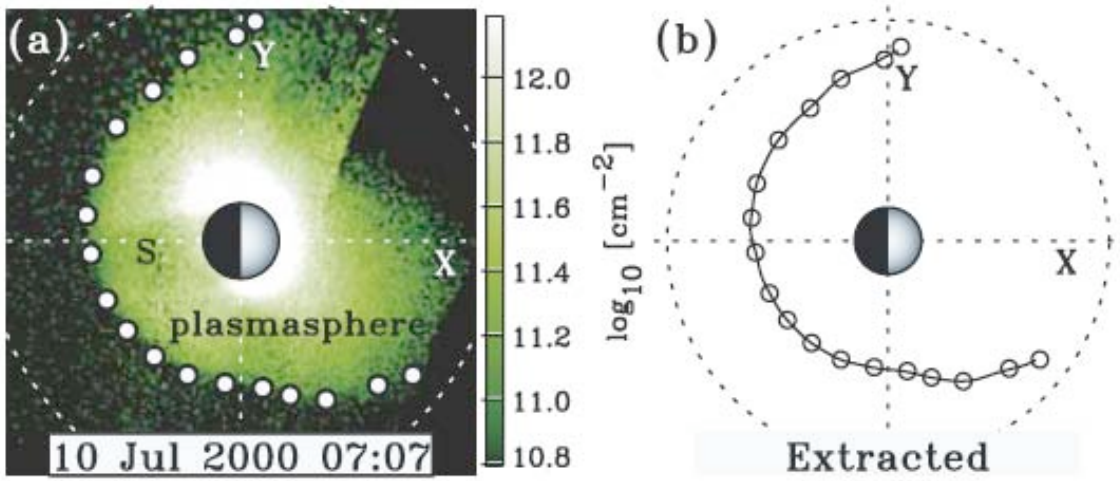

Goldstein et al., 2004

SAMPEX

- SAMPEX spacecraft:
  - polar LEO (500-620 km), operational 7/1992 to present (by NASA to 2004, then by Aerospace)
- **PET:** Proton/Electron Telescope
  - has series of eight solid state detectors
  - detects energetic electrons (0.4-30 MeV) and H^+/He^+ (18-250 MeV)
- HILT: Heavy Ion Large Telescope
  - designed for heavy ion observations, also provides 100-ms resolution data on >1 MeV electrons
- SAMPEX provides pitch angle information only when in spin mode
  - this mode periodically 5/1996-5/1998, 12/1999-2/2000
  - full pitch angle information twice per 60-sec rotation
- 8-year spectrogram of SAMPEX electron observations with Dst--

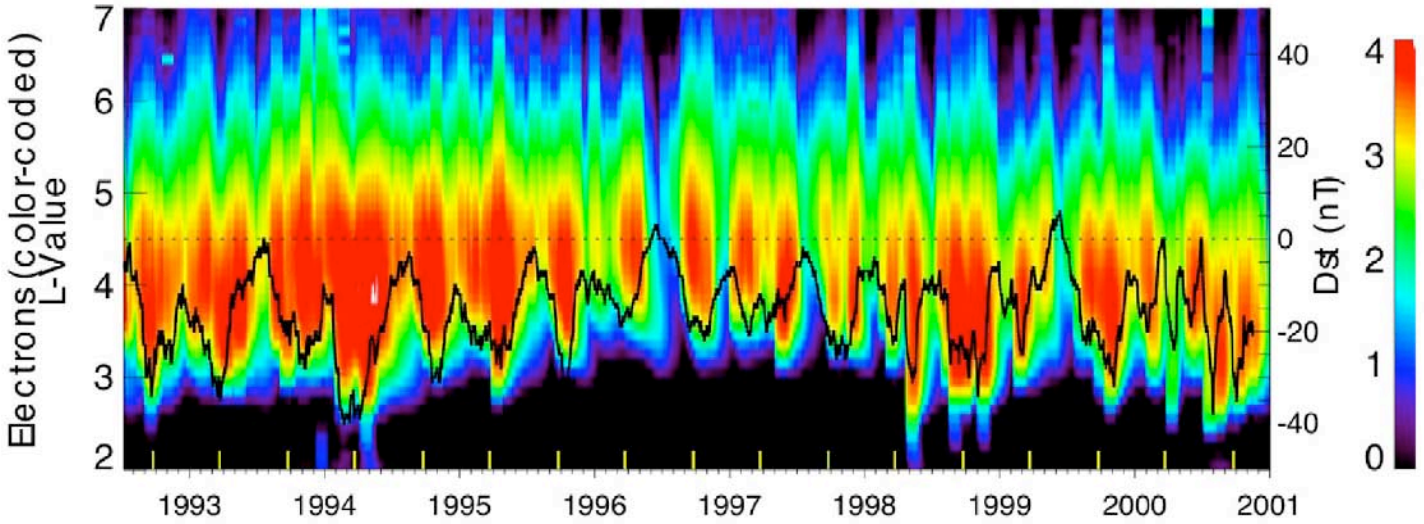

Li et al., 2001

Method and Results

Method and Results

- Results from two case studies:
  - 1 day, 18 June 2001 (day 169)
  - 72 days, 21 March-31 May 2001 (days 80-151)
  - these periods selected to match availability of processed IMAGE data (J. Goldstein)
- Further results from developing database:
  - Most of 2001
  - Individual storm events 1998-2004
- 17 months of data processed to date

- Method described in Anderson, Johnston and Goldstein (2008), *GRL*, 35:L15110.
- First results in Johnston and Anderson (2009), submitted to *JGR*.

Method: algorithm for LIT ID

- [1] use DMSP [H^+] data from 20-65° MLAT N/S
- [2] smooth data with Hanning window with fixed MLAT width
- [3] if maximum dynamic range is less than a factor of 10, ignore pass
- some passes rejected manually (too noisy, no LIT, etc.)
  - typically LIT not observable in DMSP data for SZA < 95°

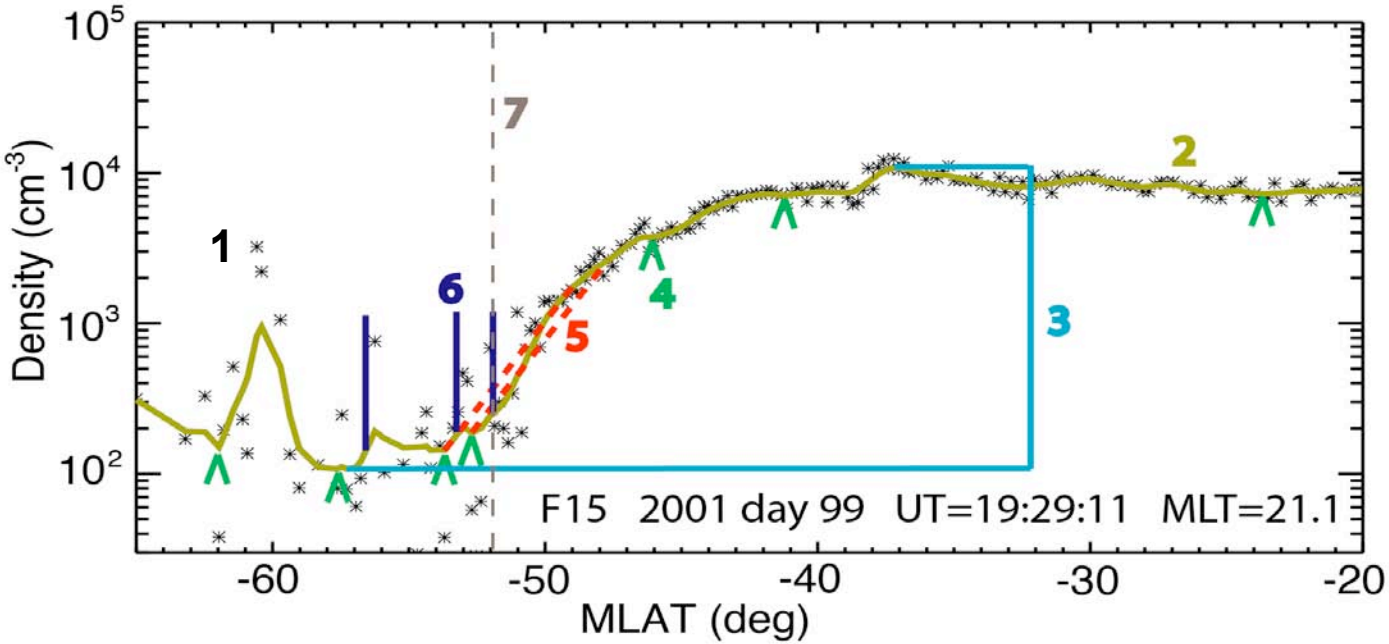

Method: algorithm for LIT ID

- [4] identify all local minima in smoothed density
- [5] identify subset of minima with steep equatorward rise in density
- [6] move equatorward to location where density is factor of *F* greater than at minimum (*F*=1.3)
  - *F* value chosen to avoid bias from broad minima (mean ΔMLAT ~ 1°)
- [7] manually identify one such location as PP

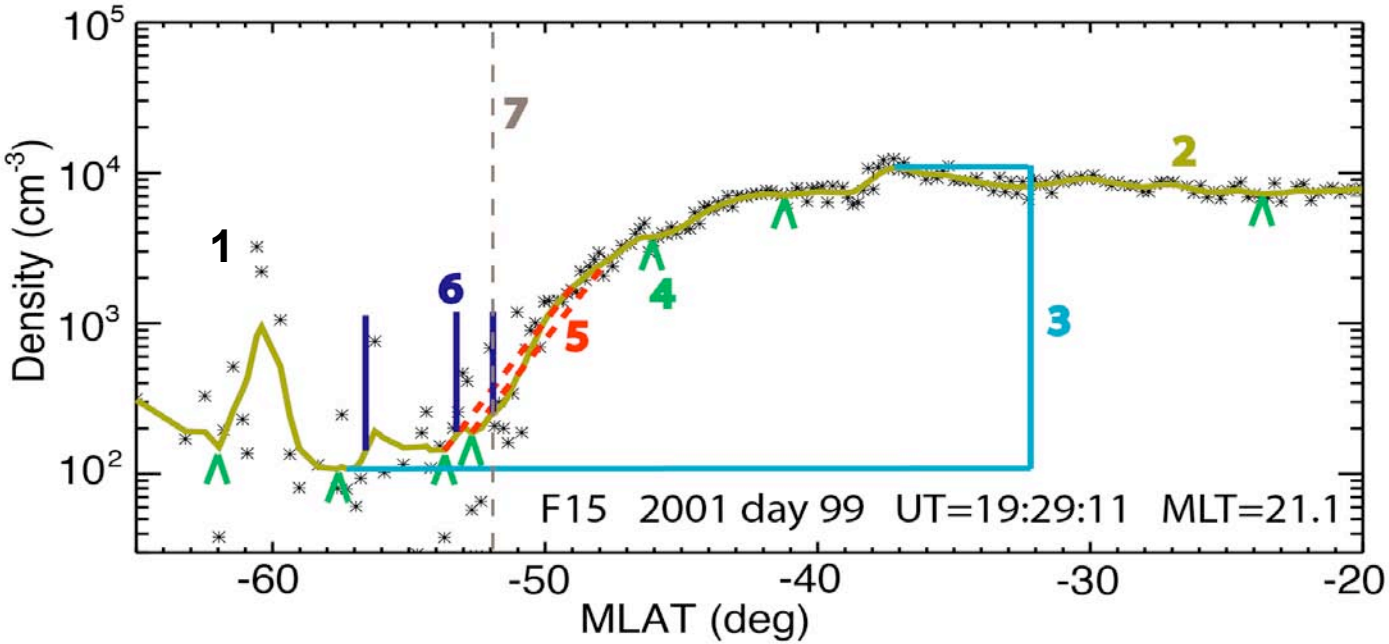

Method: mapping to equatorial plane

- Map plasmapause ID along field lines from DMSP location to equatorial plane
- Use both internal and external fields from GEOPAK
  - internal: epoch-appropriate IGRF
  - external: Tsyganenko 2001 (with ACE data for input)
- Figure shows orbit track from one DMSP pass mapped to SM X-Y plane with (red) and without (dark blue) external field
- Note that mapping is not required for DMSP-SAMPEX comparisons (both in LEO)

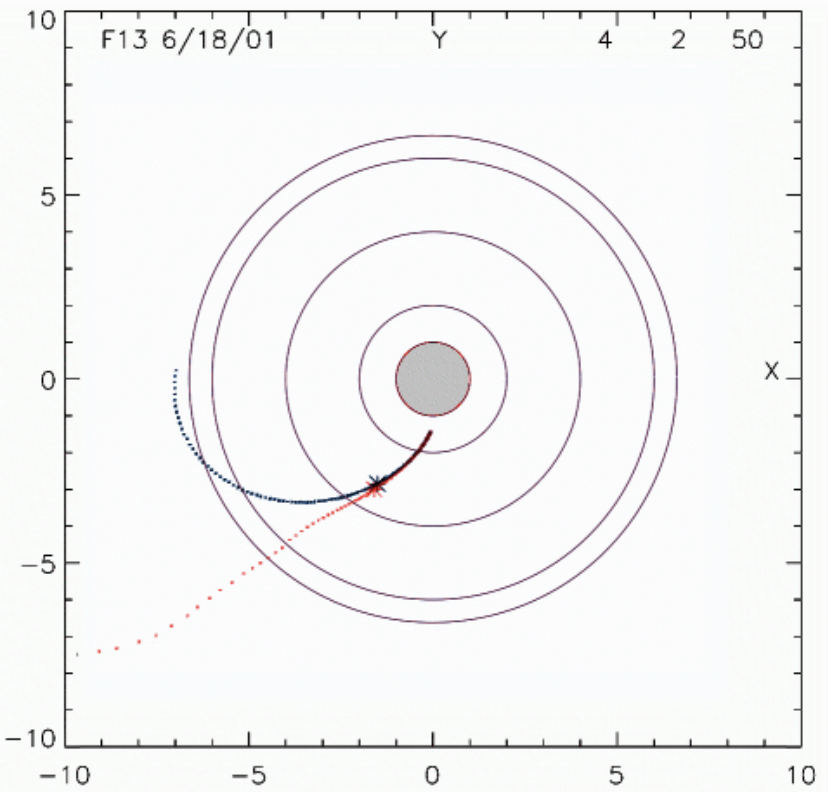

Results: LIT identifications

- Plots show DMSP H^+ density vs. MLAT, smoothed density in green
  - pre-midnight on left, morning on right
- Vertical red line is equatorward electron precipitation boundary
- Semi-automatic PP identification is at blue line

18 June 2001

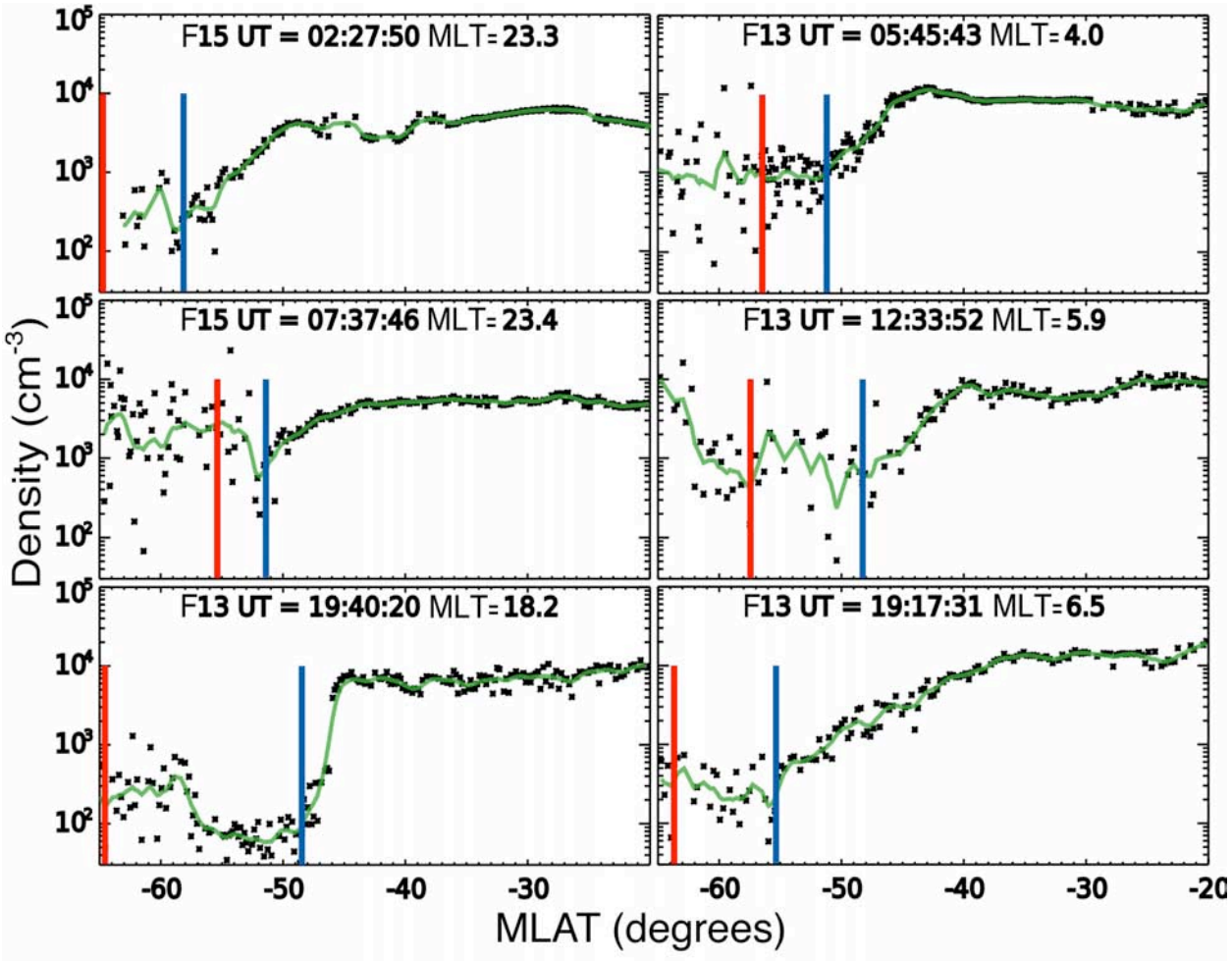

Results: mapped IDs from 1-day study

- For 18 June 2001, plots show IMAGE EUV images of plasmasphere projected to SM X-Y plane, Sun at right
- Red lines show mappings of DMSP orbit track to SM X-Y plane, red cross shows identified plasmapause

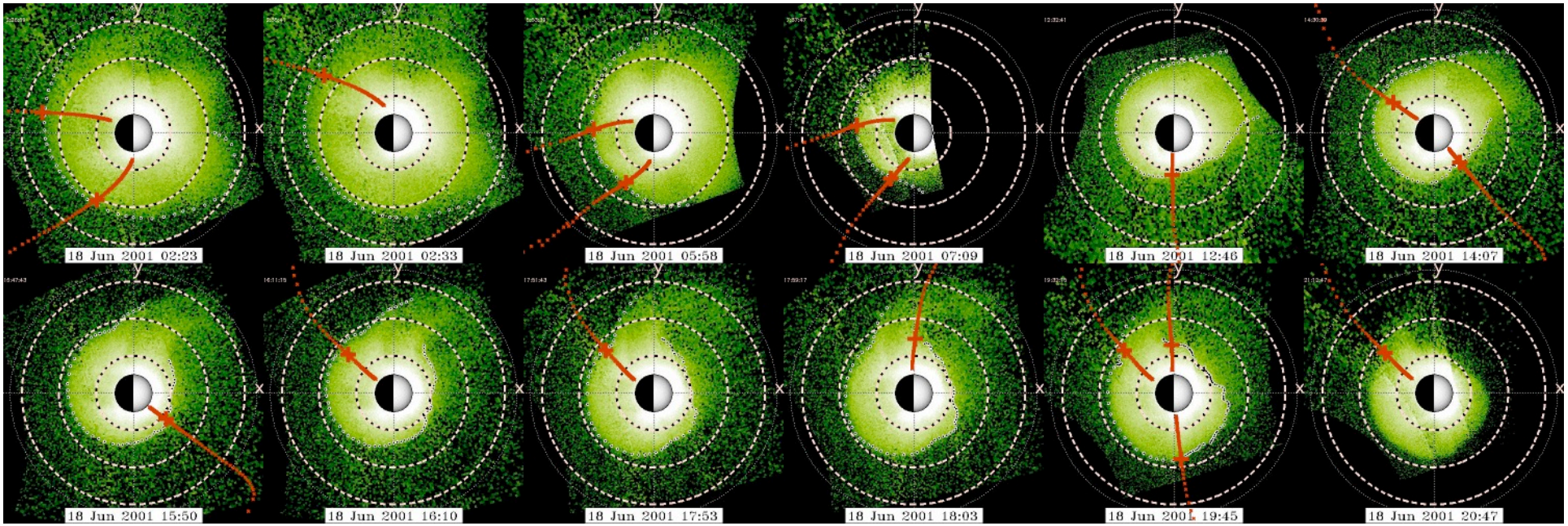

Anderson, Johnston, and Goldstein, 2008

Results: IDs from 72-day study

- Statistics for 72-day study (2001 days 80-151):

all passes	15,268 (100%)
rejected by program (dynamic range too low)	5,253 (34.4%)
rejected manually before analysis (data too noisy, no visible LIT)	7,622 (49.9%)
rejected manually after analysis	40 (0.3%)
retained plasmapause IDs	2,353 (15.4%)

- Average of 33 plasmapause IDs per day (range 3-64)

Results: IDs from 72-day study

- DMSP orbit orientation imposes preferred MLT distribution
  - dusk-dawn or 0930-2130 at equator
- For LIT to be identified, must have >~5% H^+ -- i.e. be near or above O^+ transition height
  - strong SZA dependence (SZA>~95°)
  - winter and/or nightside passes preferred
- Mapped MLT (angle from sunward in SM equatorial plane) is further affected by anti-sunward stretching of B field lines at high altitudes

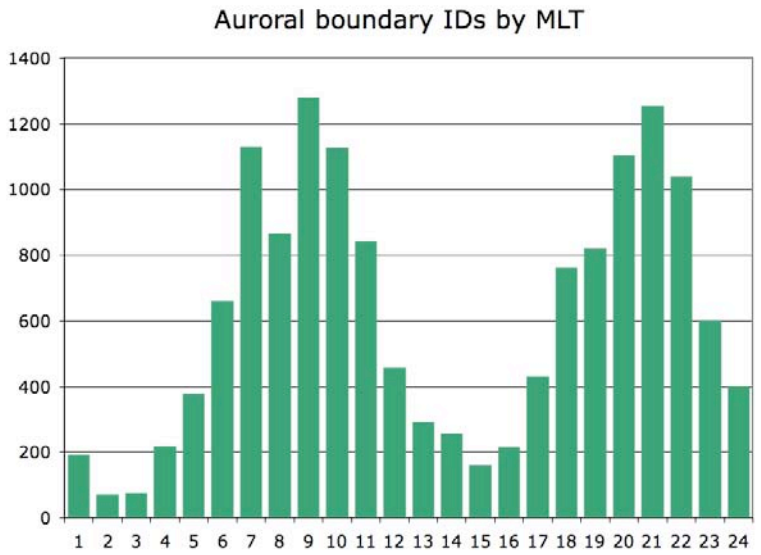

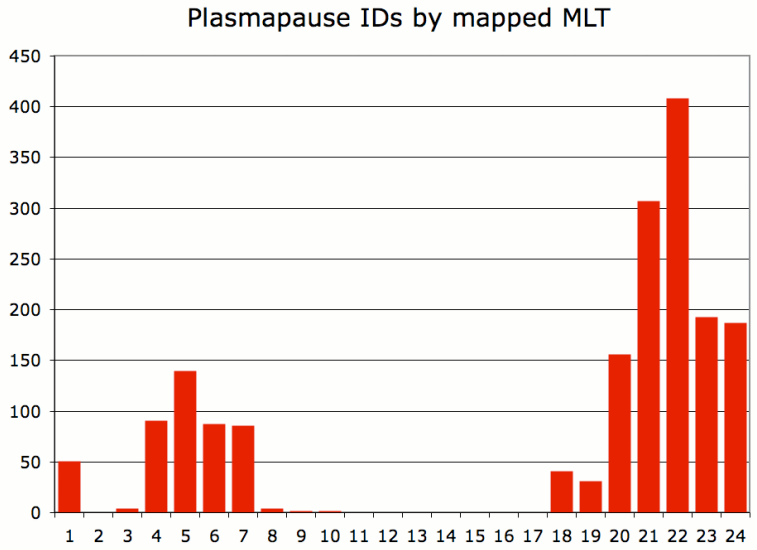

Results: comparison to IMAGE

- 72-day study yielded 187 comparisons to IMAGE
- two clusters in data:
  - "good" match cluster, N=145 (78%), mean difference 0.435±0.407 L
  - "mismatch" cluster, N=42 (22%), mean difference 1.770±0.440 L
  - mismatch defined by $(L_I-L_D)/L_I > 0.41L_I$
- examination of mismatches suggests DMSP RPA data is showing plasmasphere structures (plumes, notches, etc.)

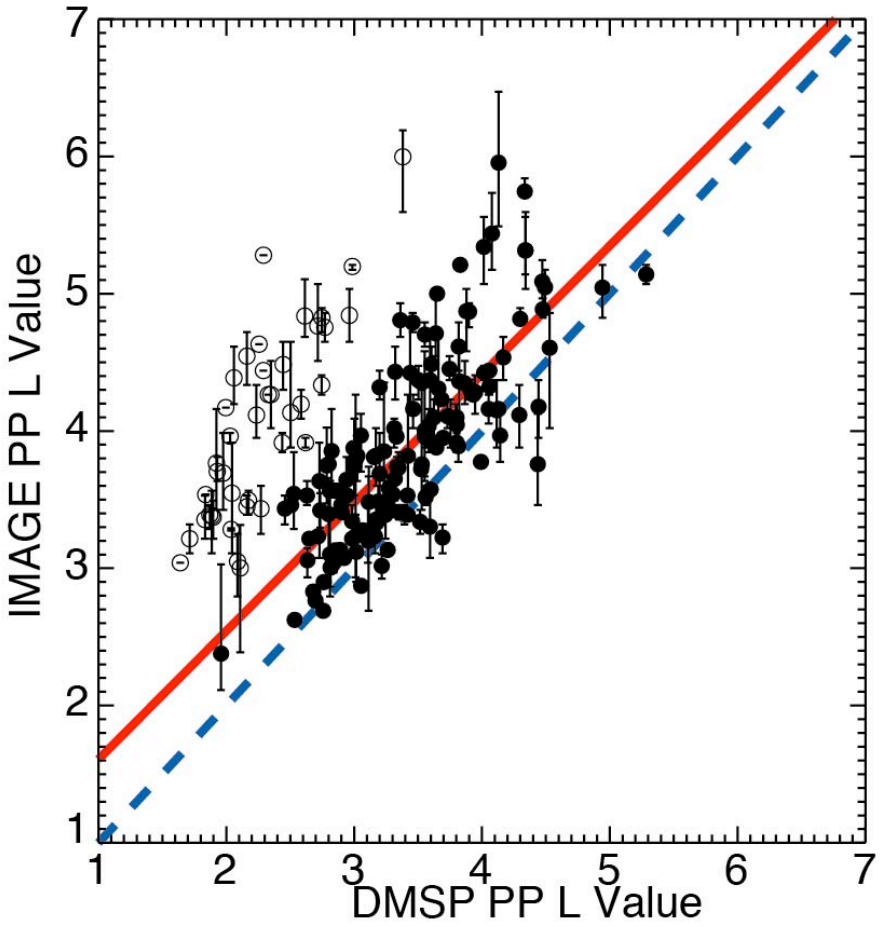

Anderson, Johnston, and Goldstein, 2008

Results: mismatch investigation

- four H^+ density plots in 50-min period on 29 May 2001: three good matches, one mismatch (F15)
  - IMAGE EUV shows mismatch case maps to inside of plume
  - DMSP RPA data shows clear LIT in good cases, suggests plasmasphere structure in mismatch case

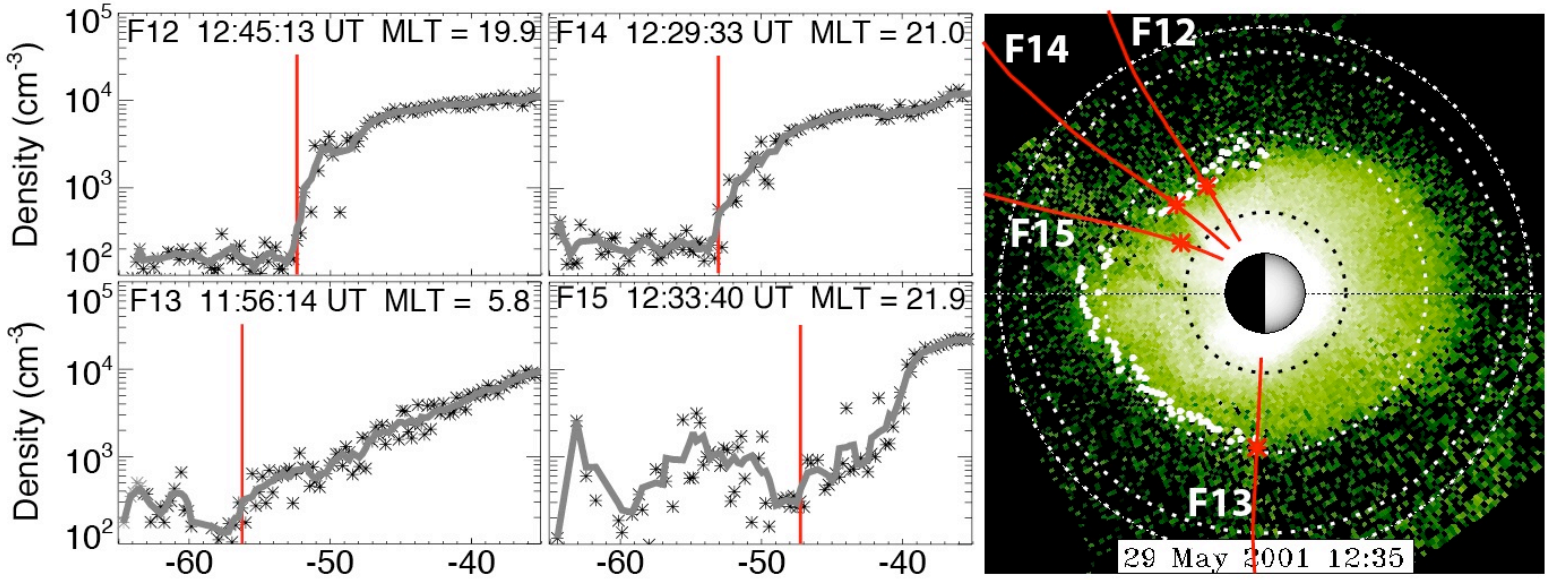

Anderson, Johnston, and Goldstein, 2008

Results: comparison to PP model

- comparison to O'Brien- Moldwin model (2003, *GRL*, 30:1152), parameterized by Dst and MLT
  - Model based on CRRES observations
- model PP averages 0.893±0.602 L greater than DMSP PP
- for L>~4, results diverge
  - model may not extend to Dst ~ 0
  - DMSP ID method may have difficulty with diffuse plasmapause, tends to cut off at L~5

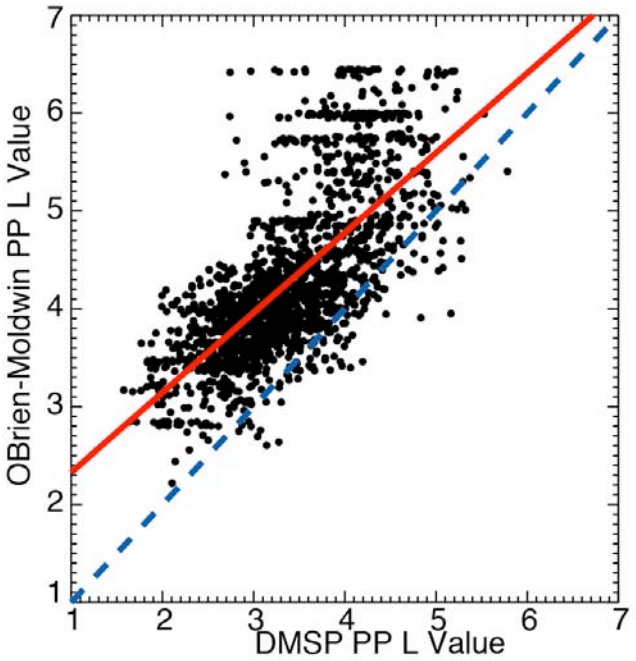

Anderson, Johnston, and Goldstein, 2008

$$L_{pp} = -1.54\left[1 - 0.04\cos\left(\frac{\mathrm{MLT} - 20.6}{24/2\pi}\right)\right]\log_{10}|\mathrm{Dst}| + 6.2\left[1 + 0.04\cos\left(\frac{\mathrm{MLT} - 22}{24/2\pi}\right)\right]$$

Results: microbursts

- red: SAMPEX-identified microbursts
- green: all DMSP-based plasmapause IDs (daily average in black)
- shows strong correlation in radial dynamics
  - microbursts nearly always outside PP (all but 5 of 2170)
  - during erosion, inward movement of microbursts follows inward PP move-ment within hours

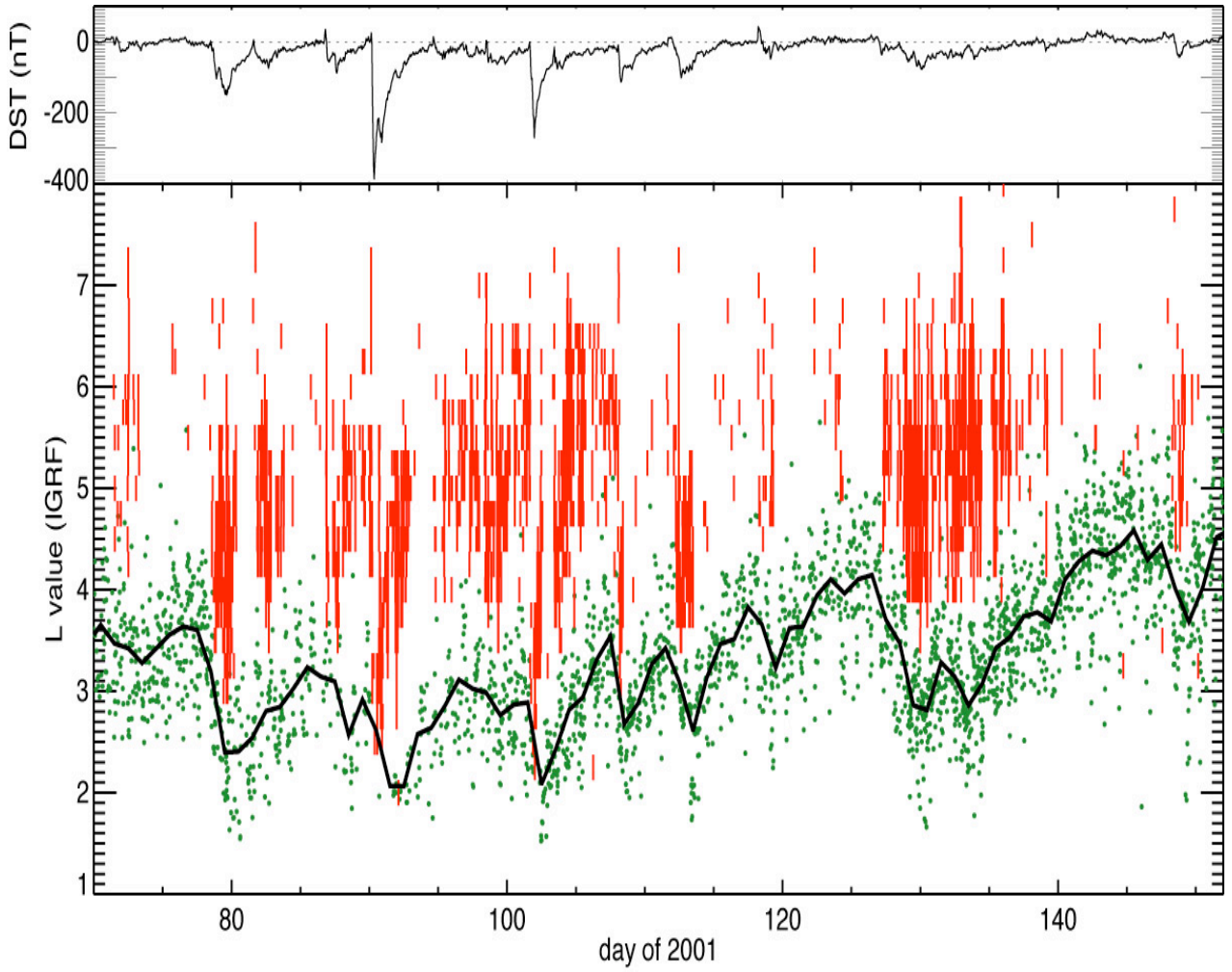

Johnston and Anderson, 2009, submitted to JGR

Results: superposed epoch study

- Superposed epoch study of 7 storms, Dst_{min} -100 to -250 nT
- plasmapause IDs (green) with 12-hr average (black), microburst locations (red) (MLT 0-9 hrs)
- Dst (top) and microburst frequency (below)
- Shows microbursts intensify and move inward within hours of storm
- Intense microbursts last 1-2 days from Dst_{min}, relatively little activity not associated with storms

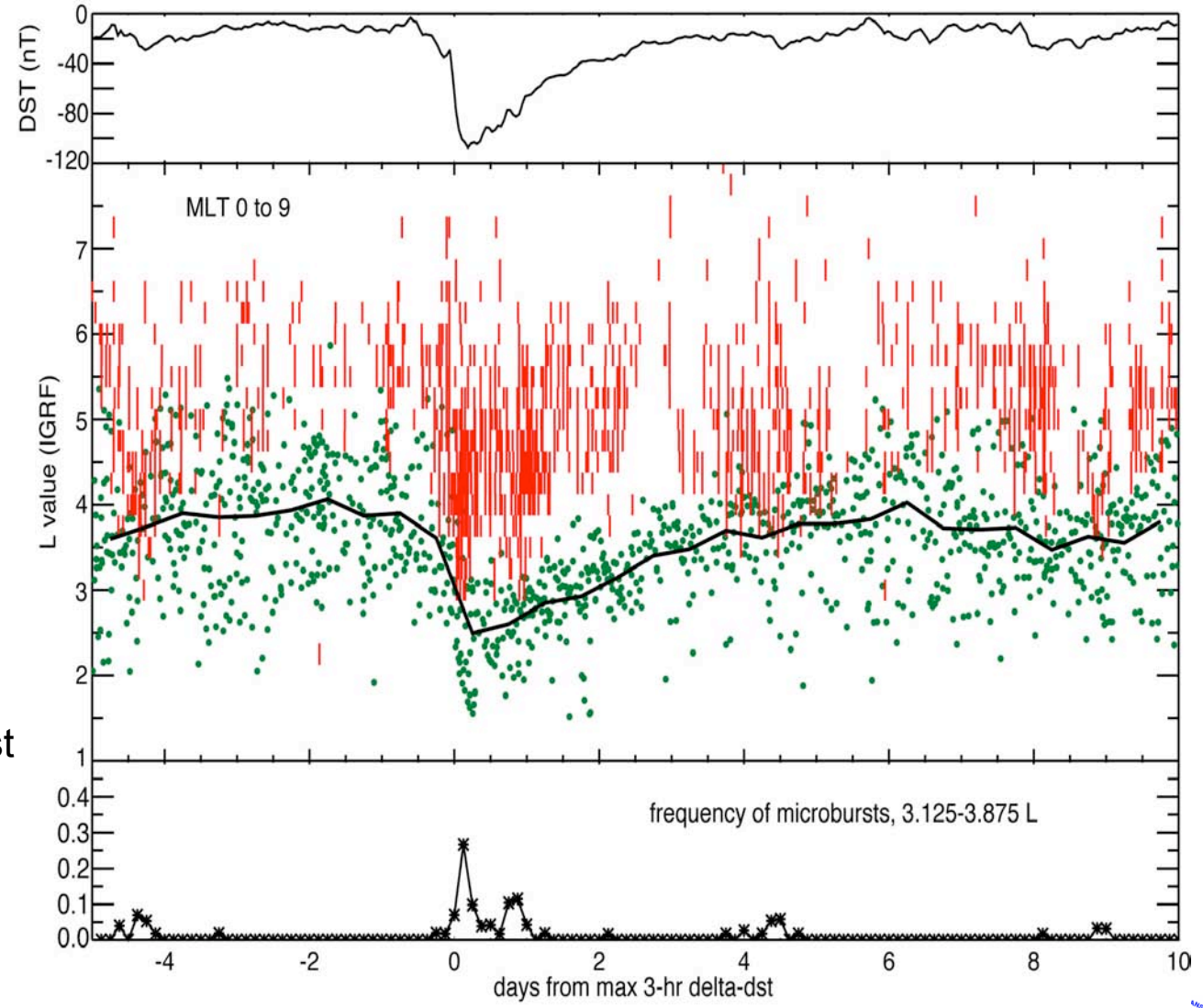

Johnston and Anderson, 2009, submitted to JGR

Results: microburst delay times

- Histograms show binned counts of PP and microburst detections in time relative to Dst_{min}
  - each plot shows one 0.25-L bin
  - includes microbursts in bin, PP in bin or outward
- Shows microbursts occur at L-values within hours of emptying by plasmasphere erosion
- Delays range from <2 hrs at L=3-3.25 to 6-8 hrs at L=4

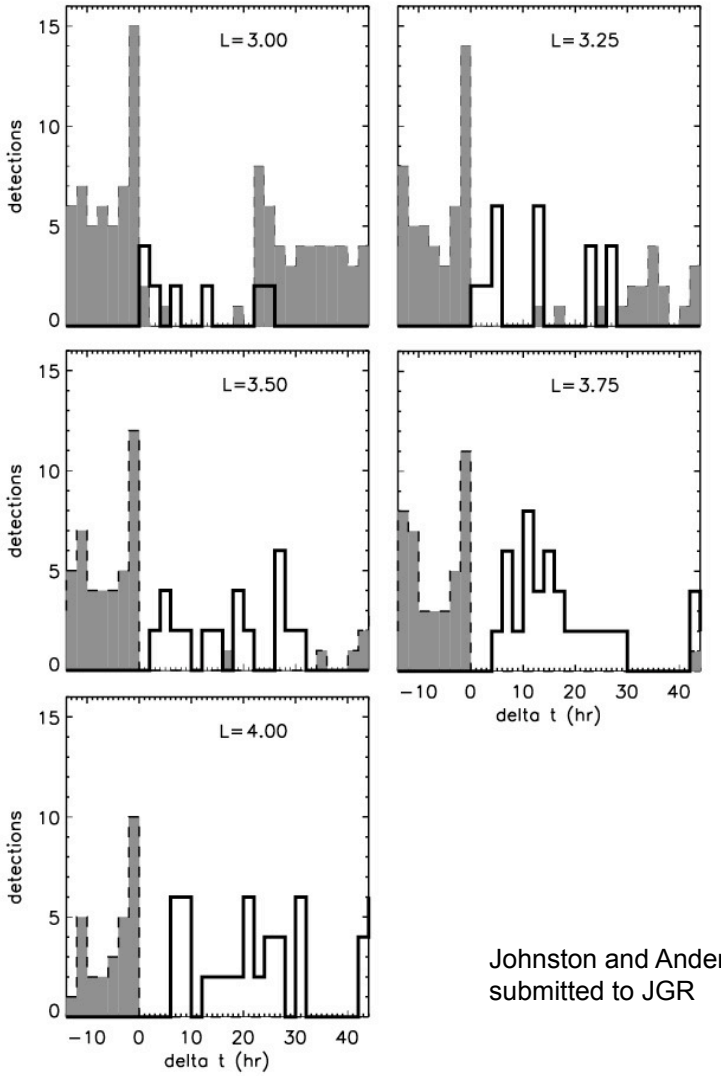

Johnston and Anderson, 2009, submitted to JGR

Cause of microbursts

- Given occurrence of relativistic microbursts at low L-values within hours of plasmasphere erosion, if this is chorus-driven it requires:
  - Injections of soft electrons as source of whistler chorus;
  - Development of chorus itself;
  - Presence of relativistic electron flux to be scattered by chorus
    - either already at these L-values, radially transported, or newly energized

Results: microbursts

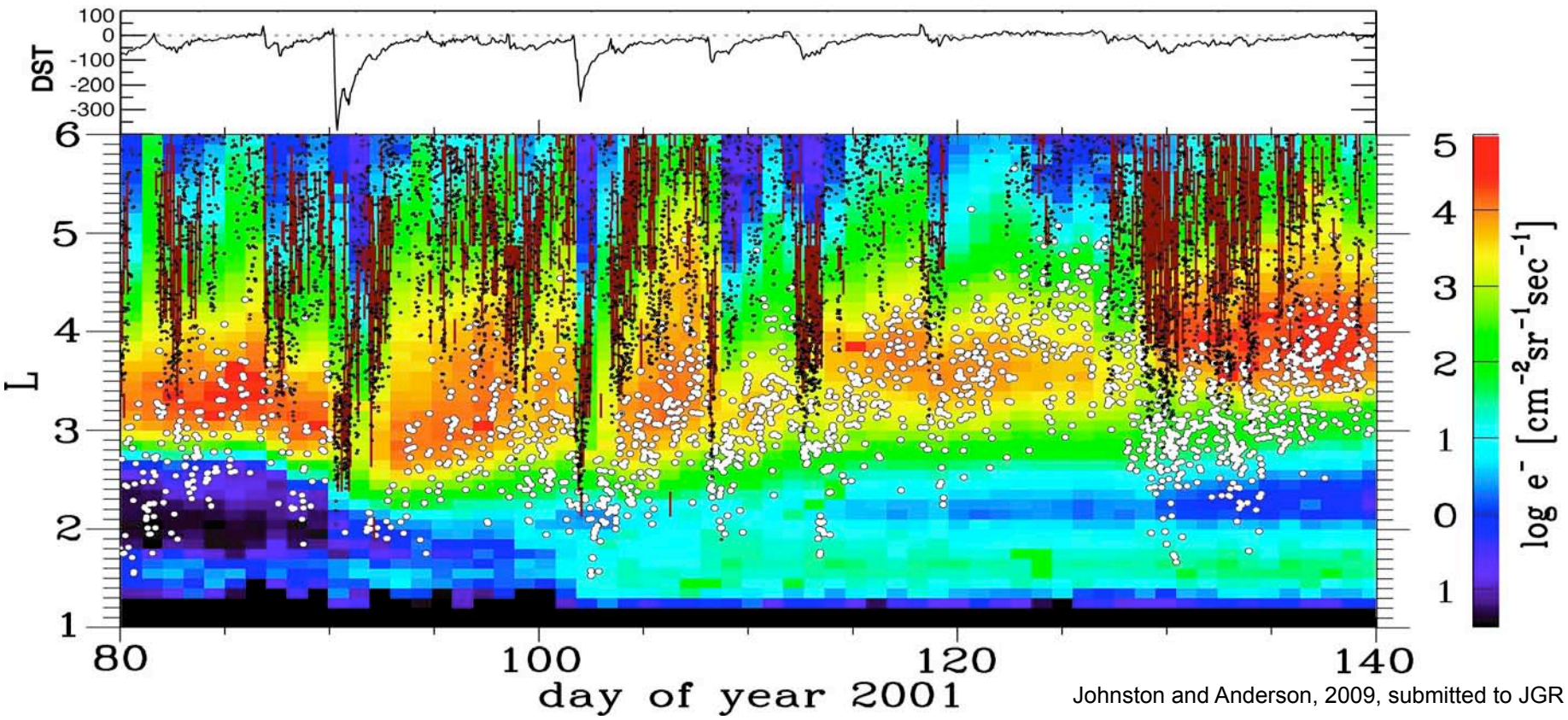

Johnston and Anderson, 2009, submitted to JGR

- Plot shows spectrogram of radiation belt flux (2-6 MeV e^-)
- Dark red lines: L-value bins with detected microbursts
- White dots: PP detections
- Black dots: inner edge of plasmasheet precipitation

Results: microbursts

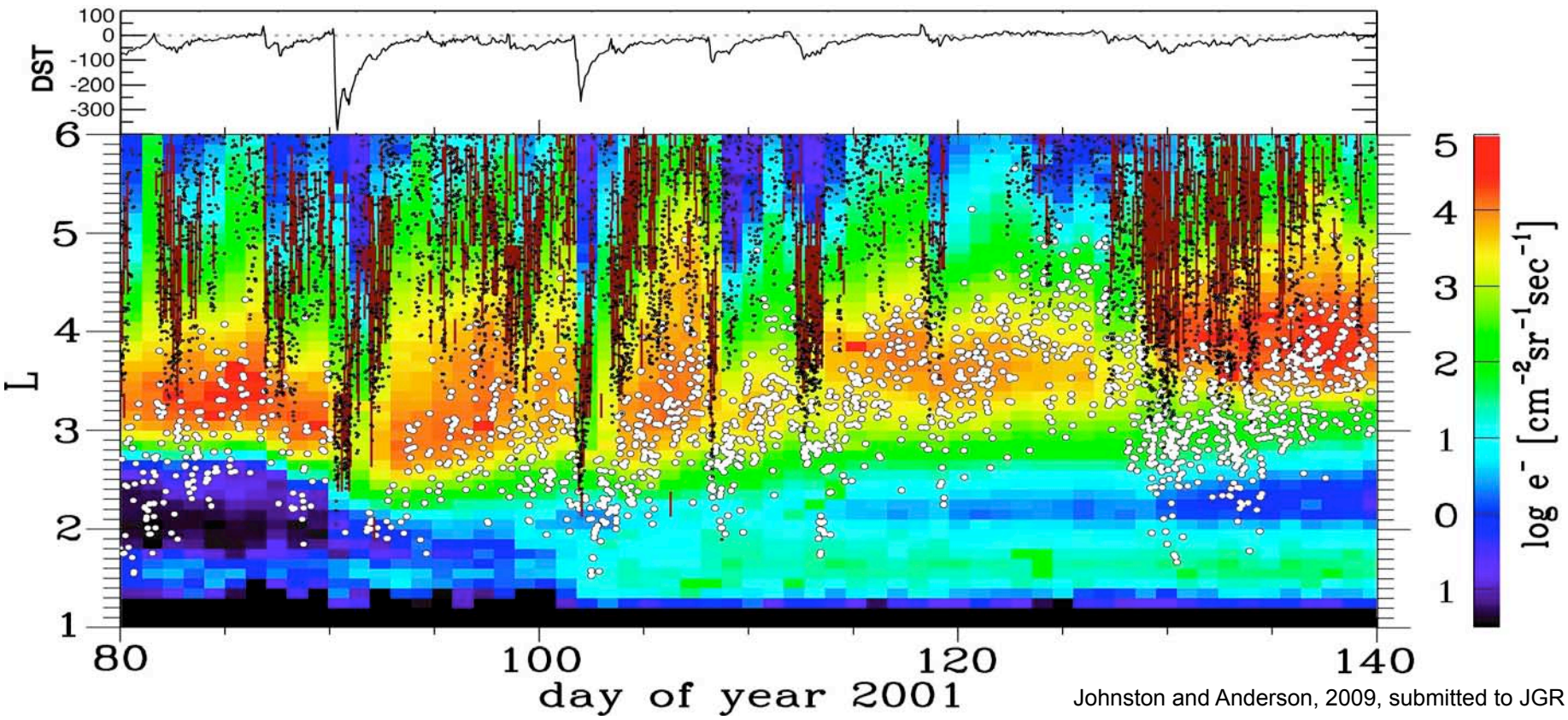

Johnston and Anderson, 2009, submitted to JGR

- Shows correlation between plasmasheet and microbursts combined with radiation belt flux
- Consistent with microbursts resulting from chorus interactions, chorus triggered by plasmasheet injections (Li et al., 2009)

Microbursts vs. plasmasheet/RB flux

- Plots show microburst frequency vs. log electron flux (horiz.) and L-value relative to innermost plasmasheet detection (vert.)
- Binning by 12 hrs (top), 6 hrs (bottom)
- Results:
  - Hardly any microbursts inward of plasmasheet
  - Microbursts increase with higher RB flux and more plasmasheet overlap
  - Drop in microbursts at upper right may be poor statistics

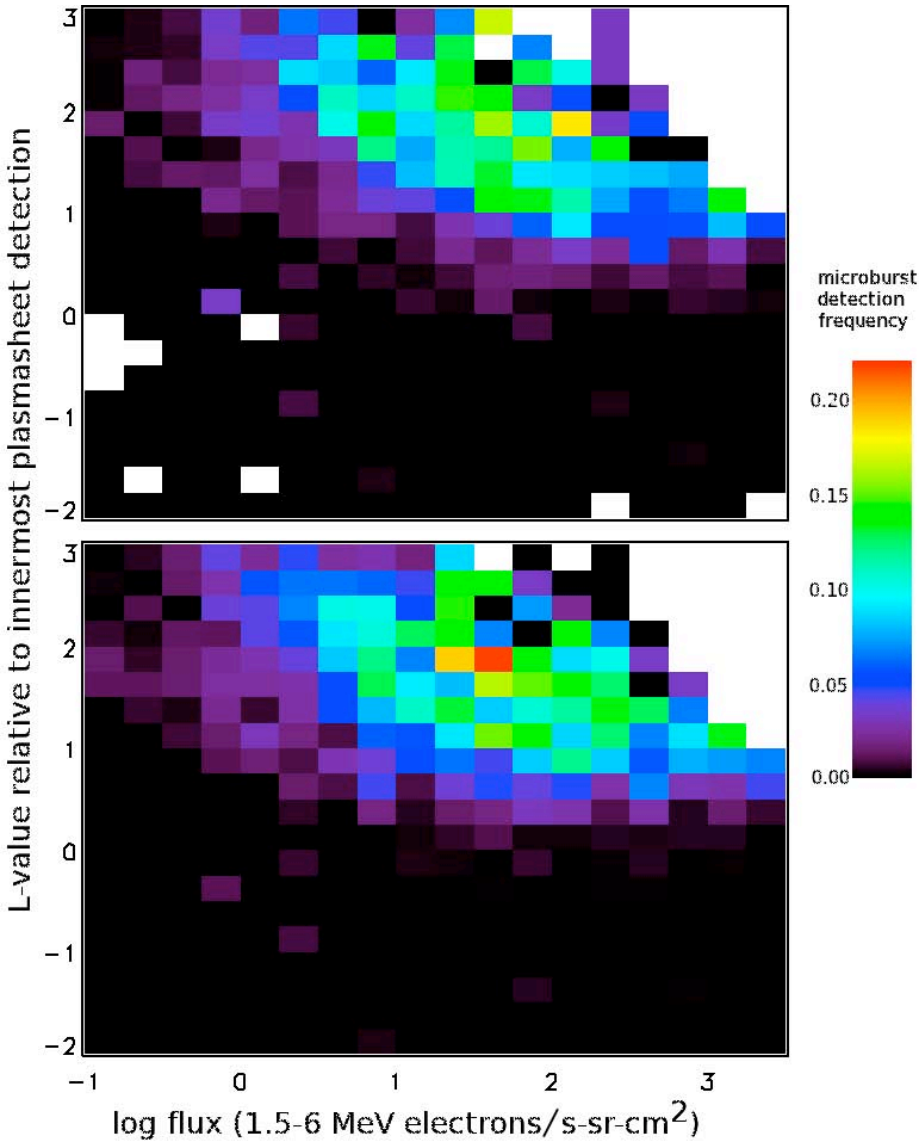

Radiation belts and plasmapause

- Spectrogram of daily average electron flux (2-6 MeV)
- Daily average PP location with standard deviation (white)
- Storms produce prompt changes in RB, usually depletion, with slower recovery often at different L-values
- Plasmasphere erosion, refilling seen

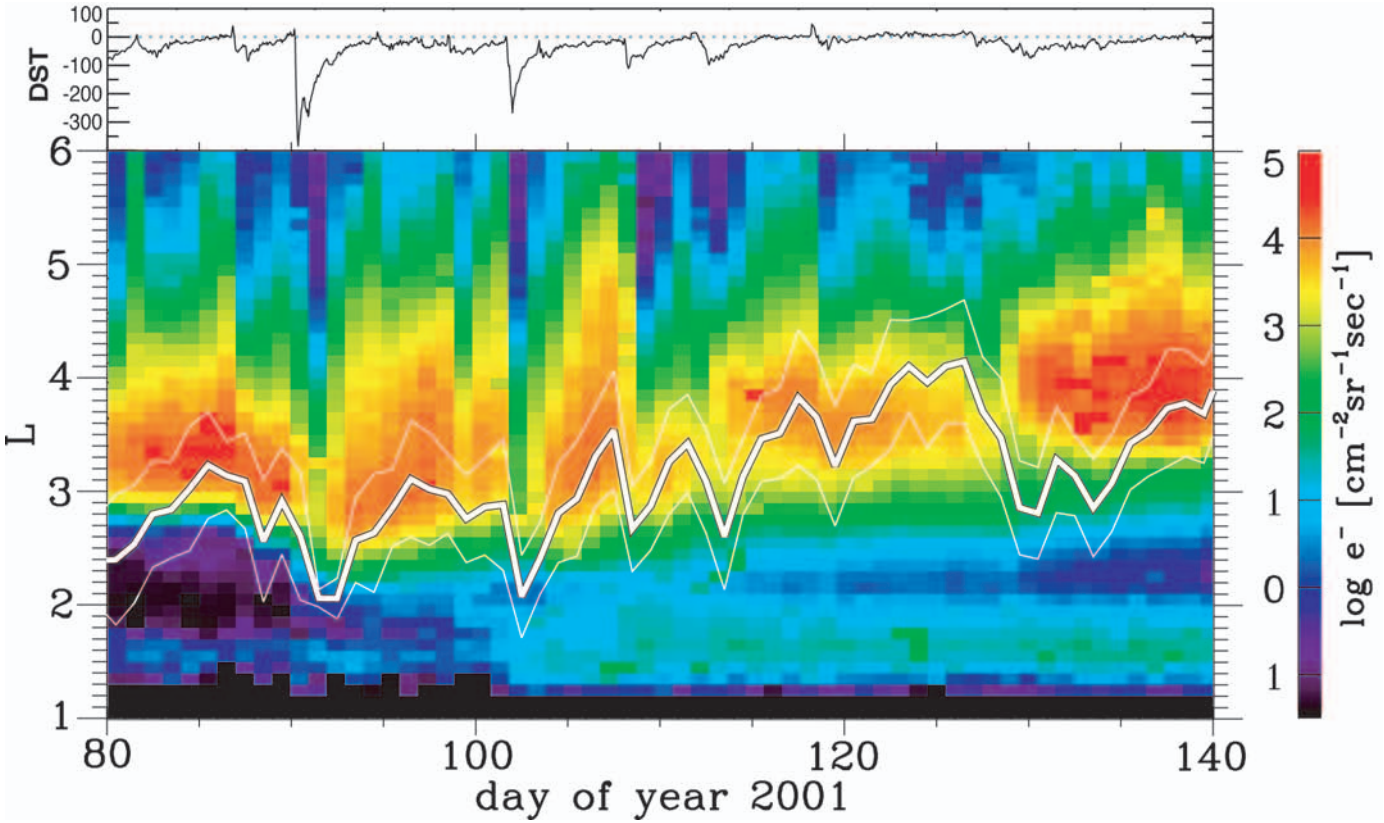

- Note that RB recovers outside PP, but when PP recovers to overlap RB this appears to be accompanied by slow RB losses

Radiation belt response vs. plasmapause

- Analysis method:
  - average RB flux by 1 day, 0.1L bins
  - Find ratio of each bin's flux to flux one day earlier
  - Collect results by L-value relative to PP and by Dst (2-day mean, bins of 50 nT)
  - Median results from 82 days
- Results
  - Mean PP location L=2.1-3.7
  - Outside PP, flux tends to increase, more with high Dst
  - Inside PP, far less change, flux decreases at lower Dst
- Bottom line: RB flux dynamics changes at PP

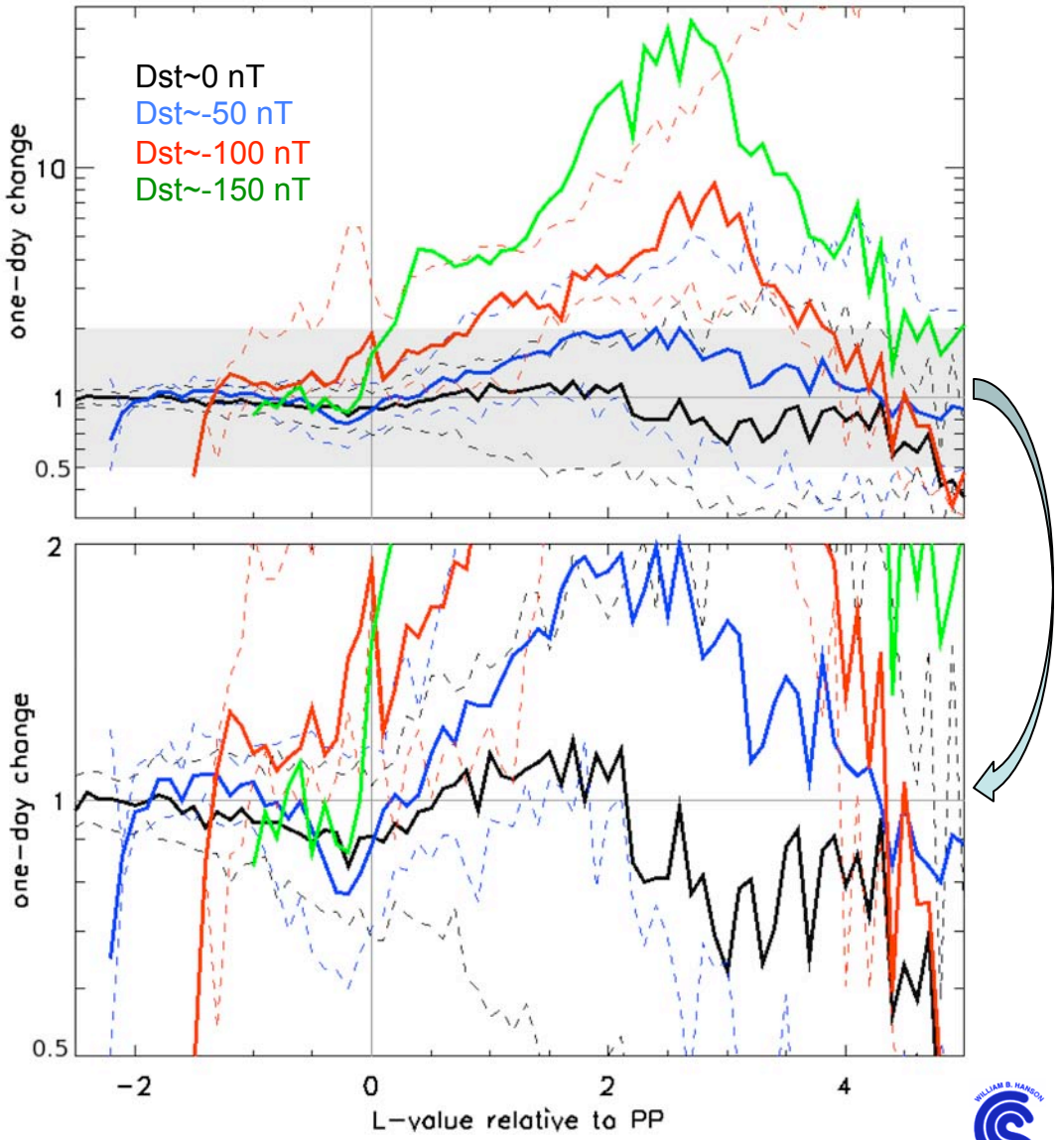

Radiation belt response timescales

- Same results but expressed as e-folding timescales: $e^{\pm t/T}$
  - Increases *
  - Decreases <>
- Shows trend for increasing RB flux outside PP, greater increase with higher Dst
  - Peak ***T*** ~10 days for Dst~0 nT
  - Peak ***T*** ~8 hrs for Dst~-150 nT
- Decreasing flux typical inside PP
  - ***T*** ~10 days at low Dst
  - Flux increases at high Dst, but far below rates outside PP
- Results poorly resolved for ***T*** >10 days
- Significant change at PP location

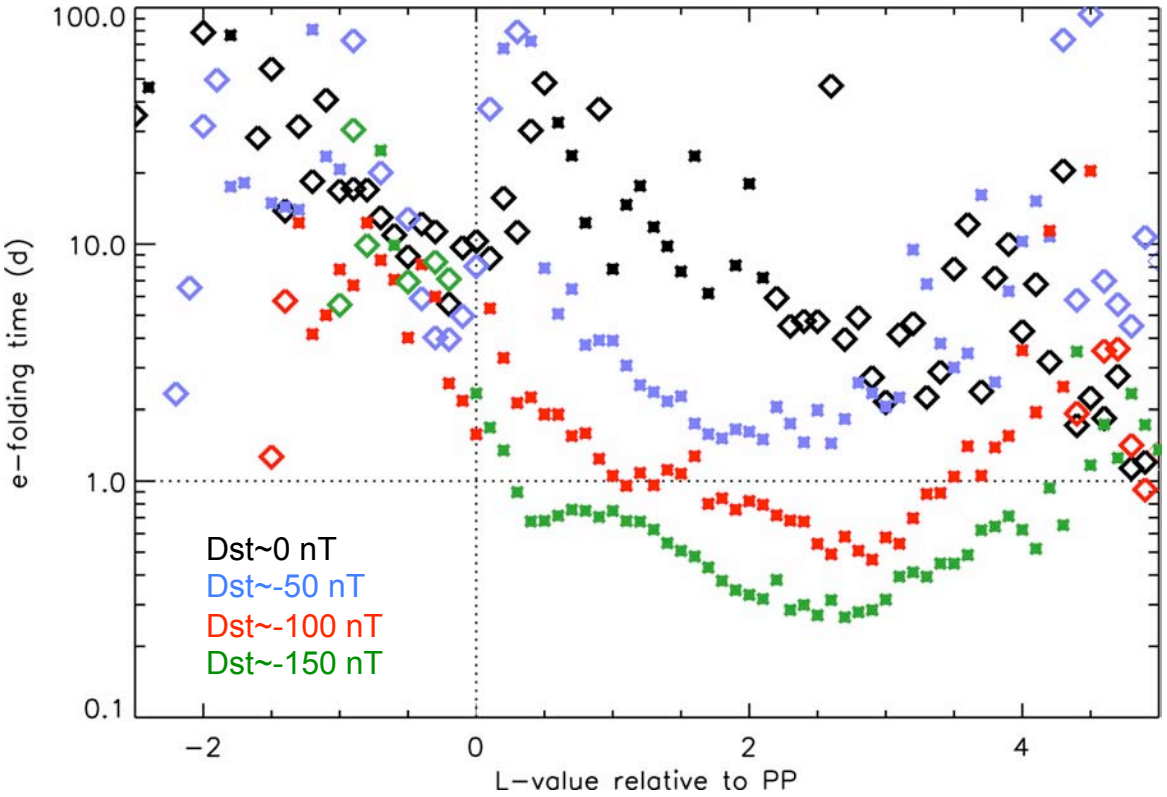

Dst range (nT)	-175 to -150	-125 to -75	-75 to -25	-25 to +25
Days	1	5	26	50
Mean PP	2.07	2.31	2.89	3.68
PP range	2.07	2.06-2.61	2.40-3.31	2.64-4.59

Conclusions

- We have obtained initial results from a method of identifying the plasmapause using DMSP observations of the LIT.
- Comparisons show good correlation with IMAGE plasmapause IDs and O'Brien-Moldwin model.
- Initial results from comparisons to SAMPEX microburst observations show microbursts follow plasmasphere erosion on timescales of a few hours
- Comparisons to SSJ/4 observations support association of microbursts with combination of plasmasheet injection-induced chorus plus radiation belt flux
- Analysis of radiation belt flux changes relative to plasmapause location shows expected relationship (increases outside PP, slow losses inside PP)

Continuing Research

- Build multi-year database
  - potentially over 60,000 PP IDs for 10+ years (one full solar cycle)
- Case studies/epoch analyses
  - average PP/radiation belt response to stormtime perturbations
- Study of plasmapause-LIT relationship
- Investigate obtaining high-altitude plasmasphere densities from DMSP observations
- Study of plasmapause-microburst relationship
  - place constraints on temporal, spatial dynamics
- Statistical comparison of mean PP, mean radiation belt location with time offset
  - different characteristic response times for erosion/recovery phases
- Compare wave observations (e.g. CLUSTER) to PP location
- Correlate PP location to locations/times where loss cones are populated
  - pitch angle observations available for periods in 1996-1998, 2000

Acknowledgements

- Phil Anderson
- Greg Earle, Marc Hairston, Rod Heelis, Xinchou Lou, Brian Tinsley
- Collaborators and data providers
  - J. Goldstein, T. P. O'Brien, DMSP team
- Margie Renfrow
- UTD physics faculty, staff, and students
- My parents and family
- Vickey Johnston

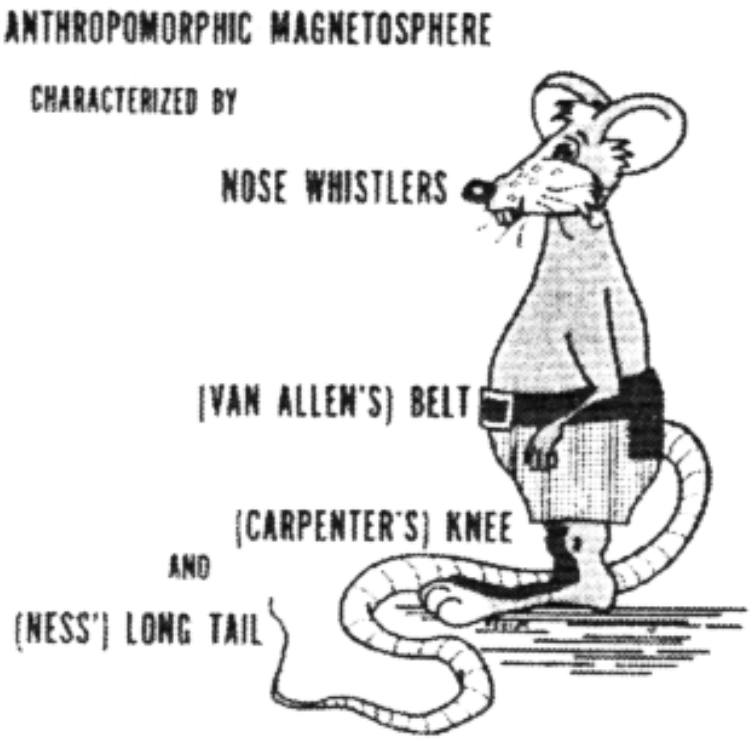

O'Brien, in Lemaire and Gringauz (1998)

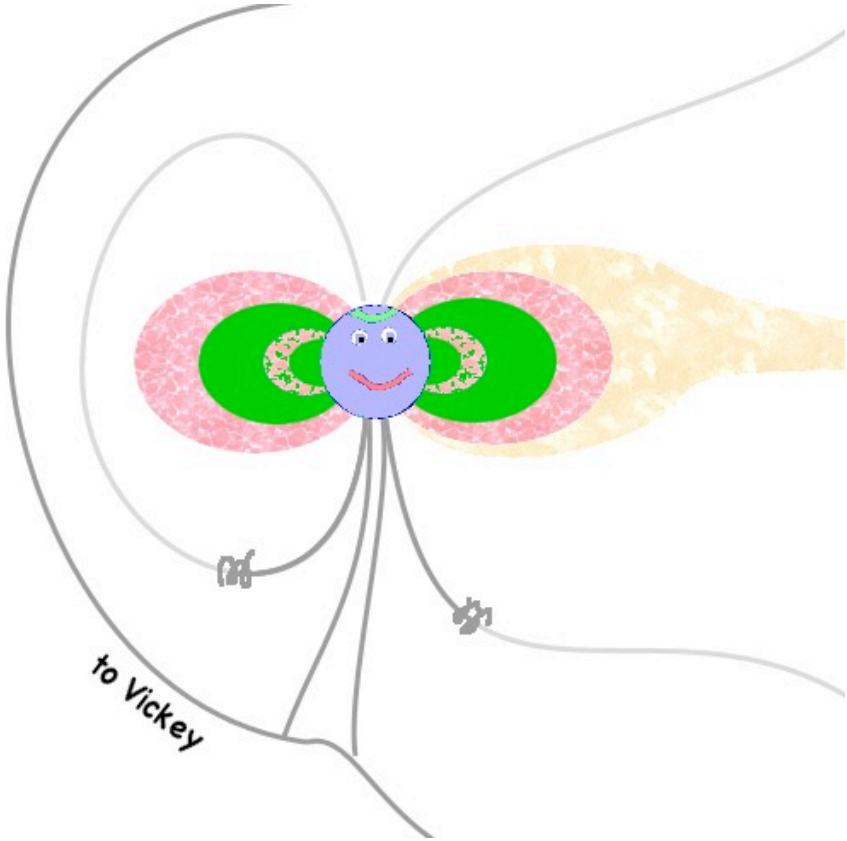

Thank you!